Fundam. Appl. Limnol. 194/2 (2020), 95–106
published online 16 November 2020, published in print December 2020

Inland blue holes of The Bahamas – chemistry and biology in a unique aquatic environment

Caroline Björnerås[1], Martin Škerlep[1, *], Raphael Gollnisch[1], Simon David Herzog[1], Gustaf Ekelund Ugge[1, 2], Alexander Hegg[1], Nan Hu[1], Emma Johansson[1], Marcus Lee[1], Varpu Pärssinen[1], Yongcui Sha[1], Jerker Vinterstare[1], Huan Zhang[3], Kaj Hulthén[1], Christer Brönmark[1], Lars-Anders Hansson[1], P. Anders Nilsson[1, 4], Karin Rengefors[1] and **R. Brian Langerhans[5]**

With 3 figures and 2 tables

Abstract: While lake systems in temperate regions have been extensively studied, tropical and subtropical systems have received less attention. Here, we describe the water chemistry and biota of ten inland blue holes on Andros Island, The Bahamas, representative of the morphological, abiotic, and biotic variation among Androsian inland blue holes. The majority of the studied blue holes were vertically stratified with oxic freshwater overlying anoxic saline groundwater of marine origin. Water chemistry (e.g. total phosphorus and nitrogen) in shallow waters was similar among blue holes, while turbidity and water color varied. Presence of hydrogen sulfide and reduced iron in and below the halocline indicate reducing conditions in all stratified blue holes. The biota above the halocline was also similar among blue holes with a few taxa dominating the phytoplankton community, and the zooplankton community consisting of copepods and rotifers. The Bahamas mosquitofish (*Gambusia hubbsi*) was present in all investigated blue holes, often accompanied by other small planktivorous fish, while the piscivorous bigmouth sleeper (*Gobiomorus dormitor*) was only present in some of the blue holes. Our field study reinforces that inland blue holes are highly interesting for biogeochemical research, and provide naturally replicated systems for evolutionary studies.

Keywords: Andros Island; anchialine caves; redox biogeochemistry; halocline, sub-tropical; aquatic ecosystems

Introduction

While extensive research on lake biogeochemistry has been conducted in temperate regions, less is known about sub-tropical and tropical systems (Fukushima et al. 2017). One such sub-tropical system is the unique inland 'blue holes' found throughout The Bahamas carbonate platform. Blue holes are water-filled, anchialine caves (Fig. 1) originating from periods of low sea level when dissolution of exposed carbonate bedrock resulted in caverns. Today the inland blue holes are commonly characterized by a surface freshwater layer overlying anoxic saline groundwater (Mylroie et al. 1995). Strong vertical stratification with a halo-

Authors' addresses:

[1] Lund University, Aquatic Ecology, Department of Biology, Lund, Sweden

[2] University of Skövde, School of Bioscience, Skövde, Sweden

[3] Chinese Academy of Sciences, Institute of Hydrobiology, Wuhan, People's Republic of China

[4] River Ecology and Management Research Group RivEM, Department of Environmental and Life Sciences, Karlstad University, Sweden

[5] North Carolina State University, Department of Biological Sciences and W.M. Keck Center for Behavioral Biology, Raleigh, USA

* Corresponding author: martin.skerlep@biol.lu.se

DOI: 10.1127/fal/2020/1330 E. Schweizerbart'sche Verlagsbuchhandlung, 70176 Stuttgart, Germany, www.schweizerbart.de

cline in the transition between fresh and saline water is maintained due to the absence of strong water currents and wind mixing. Similar anchialine limestone cave systems can be found throughout the Caribbean, the Balearic Islands, and Sardinia in the Mediterranean, as well as on the Yucatan Peninsula of Mexico where they are locally referred to as "*cenotes*" (Iliffe & Kornicker 2009).

These fascinating environments were filled with water during the past approx. 15,000 years (Fairbanks 1989), and have been subject to geological and hydrological studies including investigations on past climate and sea-level changes (Mylroie & Care 1995; Whitaker & Smart 1997; Kovacs et al. 2013). Blue holes have also been identified as 'natural laboratories' for evolutionary studies, investigating phenotypic diversity, adaptation and speciation of resident organisms (Langerhans et al. 2007; Langerhans 2009; Langerhans 2017; Lee et al. 2019), as well as for reconstructing past environments using well-preserved fossils deposited in the anoxic saline waters (Steadman et al. 2007; Hastings et al. 2014; Steadman et al. 2015). Furthermore, studies have shown that anchialine caves host complex food webs and an endemic and unique fauna (Iliffe & Kornicker 2009; Pohlman 2011). However, no large-scale investigations of the general features of water chemistry and biota across a range of blue holes have so far been conducted.

As oxygenic photosynthesis is restricted to the freshwater layer of blue holes, anoxygenic phototrophs were found to be the primary producers in the halocline where oxygen is limited (Gonzalez et al.

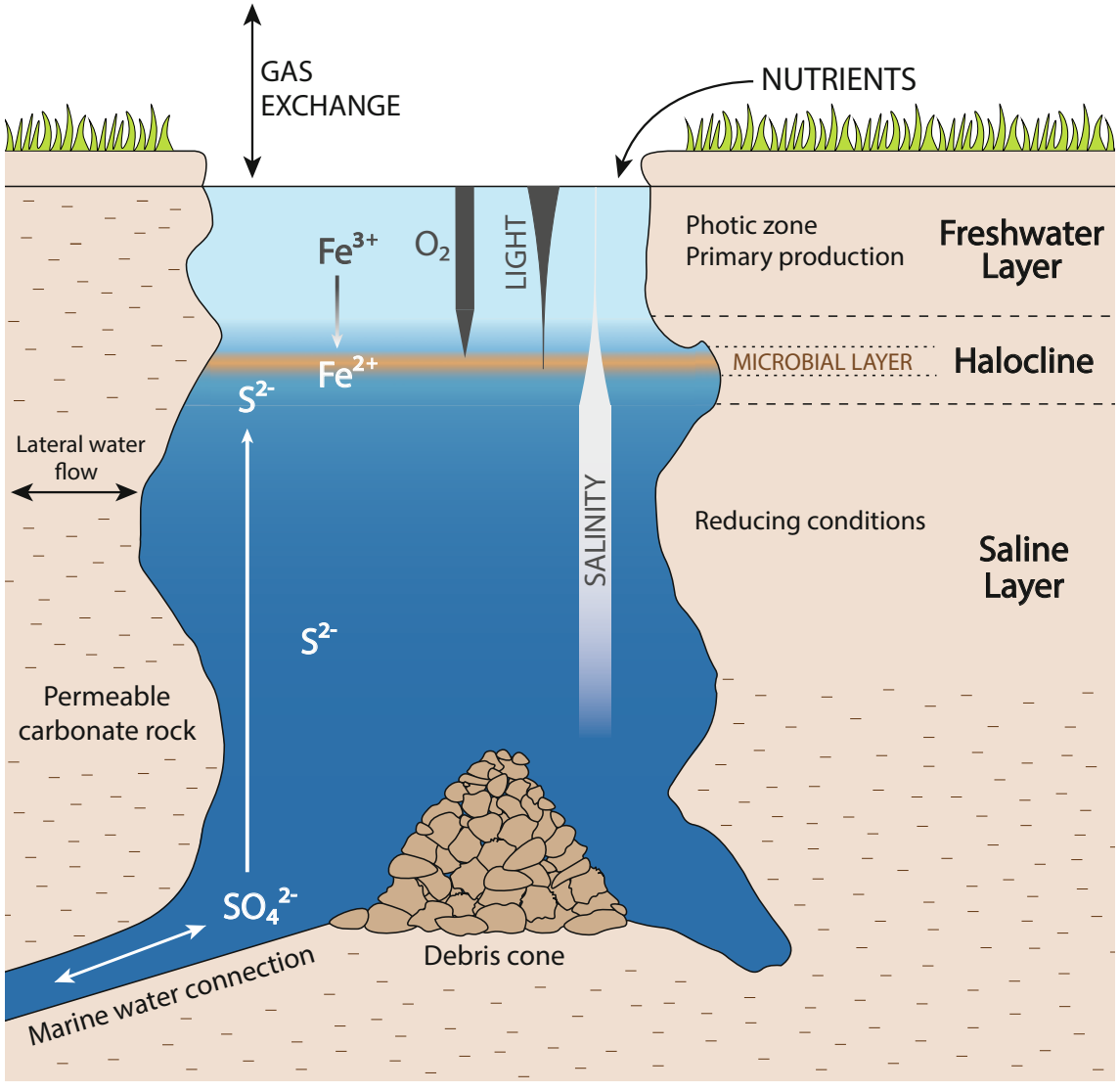

Fig. 1. Schematic figure of a blue hole including relevant physical and chemical characteristics and the possibility of deep passageways. The debris cone is a common feature in blue holes, it is created from falling debris and can vary in size and shape.

2011; Haas et al. 2018). Accordingly, the high variability in biogeochemical characteristics within and between blue holes have distinguished them as microbial hotspots (Gonzalez et al. 2011). Highly reducing conditions induced by microbial organic matter decomposition have been found in the halocline at the interface between the freshwater and saline water masses (Bottrell et al. 1991). Surface water carbon inputs drive these microbial-dominated ecosystems, where sulfate reduction is the main metabolic pathway, as is also the case in similar karst aquifers (Garman & Garey 2005). These unique conditions make studies on redox conditions and microbial metabolism highly interesting and therefore constitute a major rationale behind our study of blue holes on Andros Island.

Andros Island is the largest island in the Bahama Archipelago and harbors the greatest density of blue holes on Earth, and although chemical profiles have been described for two blue holes on the island (Bottrell et al. 1991; Gonzalez et al. 2011), we still have much to learn about biogeochemical processes in these systems. Here we provide a detailed description of the water chemistry, as well as a brief overview of the biota in 10 diverse inland blue holes on Andros Island. These sites were selected *a priori* to capture the natural variation among blue holes in morphological, abiotic, and biotic characteristics.

Methods

Site description

The Bahama Archipelago is situated southeast of the US state of Florida and northeast of Cuba and consists of more than 3000 islands in the Atlantic Ocean (Buchan 2000). Andros Island, divided into North and South, is the largest Bahamian island. The island is located on the Great Bahama Bank and has a mid to late Quaternary carbonate bedrock (John E Mylroie & Mylroie 2013). Since rainwater rapidly percolates through the porous

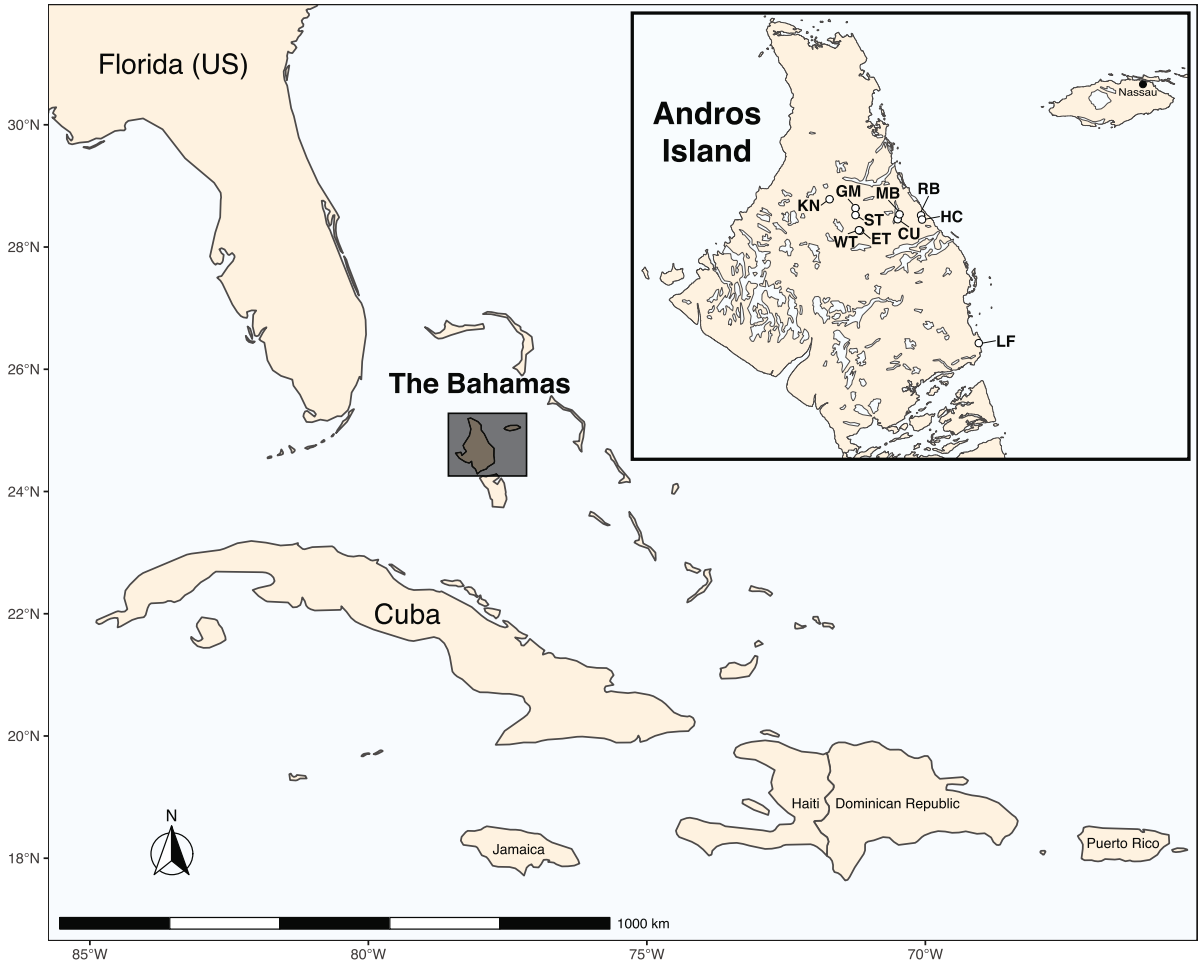

Fig. 2. Map with studied blue holes on Andros Island, The Bahamas. CU = Cousteau's, ET = East Twin, LF = Little Frenchman, GM = Gollum, HC = Hubcap, KN = Ken's, MB = Murky Brown, RB = Rainbow, ST = Stalactite, and WT = West Twin.

carbonate bedrock there are no freshwater streams and little surface water runoff on the island (Mylroie & Mylroie 2013). The climate is sub-tropical with a monthly mean air temperature ranging between 20 and 27 °C and the average yearly precipitation is 1400 mm at the island Grand Bahama situated north of Andros (Buchan 2000). The vegetation on Andros Island is dominated by pine trees and shrubs, while mangroves are abundant along the tidal shores (Smith & Vankat 1992). Here we investigated 10 blue holes distributed across North Andros (Fig. 2) within a two-week period in February and March 2018.

Field sampling

Depth profiles of temperature, salinity, dissolved oxygen (DO), and turbidity were obtained at the measured deepest point of the basin reached from the surface (disregarding cave tunnels) using a CTD probe (AAQ1186s-H; Alec Electronics, Kobe, Japan) with a 50 m cable. We measured water transparency (Secchi depth) using a Secchi disk (20-cm diameter with alternating black and white) in each blue hole. Water samples (0.5 L) were retrieved from the freshwater layer, as well as the halocline and saline layer when possible, using a MICROS water sampler (Hydro-bios, Kiel, Germany). The sampler was kept sealed until subsamples were extracted for reduced iron (Fe^{2+}) and hydrogen sulfide (H_2S) analysis, since Fe and sulfur (S) are redox active elements in inland blue holes and can be used as indicators for reducing conditions (Bottrell et al. 1991; Gonzalez et al. 2011; Haas et al. 2018). Subsampling was always completed immediately after the water was collected since Fe^{2+} and H_2S are not stable under oxic conditions.

Surveys of biota were performed using plankton nets (for phytoplankton and zooplankton), and underwater visual surveys (for fish). Phytoplankton was sampled using a 20-µm net that was pulled through the photic zone (2× Secchi depth), and a 10-µm net that was pulled through the freshwater layer. Following collection, samples were immediately preserved with Lugol's solution, and subsequently qualitatively analyzed using an inverted microscope (Nikon Eclipse TS100; Melville, NY, USA) with 200-400× magnification. The most dominant taxa based on cell number were identified and recorded. We sampled zooplankton by lowering and retrieving a 100-µm net through the freshwater layer. The concentrated zooplankton sample was analyzed qualitatively using a microscope (Dino-Lite Edge X; AnMo Electronics Corporation, New Taipei City, Taiwan) with 200× magnification and a stereomicroscope (Olympus SZX7; Tokyo, Japan). We surveyed the fish community by visually assessing fish species presence while snorkeling, a method successfully employed for these systems with a restricted volume of water suitable for fish (Heinen et al. 2013). All the observed species/taxa for both zooplankton and fish were reported, regardless of the amount of observed individuals. Several of the physical and chemical variables, as well as zooplankton and fish, have been monitored in shallow waters on multiple occasions since 2002 (R.B. Langerhans unpublished data). All observations here are consistent with prior work. Most of these data are not included here but have been used to confirm temporal repeatability (e.g. Heinen et al. 2013). We present here surface diameter measurements conducted previously by R.B. Langerhans using a Bushnell Yardage Pro Legend laser rangefinder (Overland Park, KS, USA). As most of the blue holes are roughly circular, the average surface diameter was based on two measurements: along the long axis, and along the perpendicular axis. We frequently encountered slightly different maximum depths with our CTD probe than those previously obtained by R.B. Langerhans using a drop line, and we present both values in such cases (Table 1). For Ken's blue hole, water chemistry and phytoplankton samples were not collected, due to logistical problems. Therefore only CTD probe measurements, Secchi depths, zooplankton and fish surveys are presented.

Analytical methods

Total Fe as well as Fe^{2+} concentrations were analyzed in the field shortly after sampling using the Ferrozine method (Stookey 1970; Viollier et al. 2000). The absorbance of the Ferrozine solution containing sample or standard before and after the reduction step was measured spectrophotometrically at 562 nm (DR Lange 1900; Hach, Loveland, CO, USA). To calculate Fe concentrations, sample absorbance was compared to a five-point calibration curve using a stock solution of $FeCl_3$

Table 1. Morphological and physical characteristics of the blue holes.

#	Latitude	Longitude	Surface diameter (m)	Maximum depth (m)*	Freshwater depth (m)	Secchi depth (m)
Cousteau's	24° 46′ 34.97″ N	77° 54′ 57.60″ W	68	110	19.0	8.1
East Twin	24° 45′ 05.47″ N	78° 00′ 20.70″ W	63	49.7 (61.1)	22.5	5.7
Gollum	24° 48′ 02.09″ N	78° 01′ 00.55″ W	51	13.5	13.5	4.8
Hubcap	24° 46′ 32.81″ N	77° 51′ 27.61″ W	74	18.9	10.0	4.3
Ken's	24° 49′ 11.75″ N	78° 04′ 43.14″ W	108	80.0	25.0	16.7
Little Frenchman	24° 30′ 25.13″ N	77° 43′ 19.85″ W	24	12.5†	2.0	2.7
Murky Brown	24° 47′ 13.49″ N	77° 54′ 41.65″ W	115	7.0 (8.3)	7.0	1.6
Rainbow	24° 47′ 06.00″ N	77° 51′ 36.00″ W	90	19.0 (26.0)	12.5	7.0
Stalactite	24° 47′ 07.55″ N	78° 01′ 00.37″ W	58	42.5 (54.1)	31.0	15.7
West Twin	24° 45′ 09.36″ N	78° 00′ 30.89″ W	69	15.0 (21.6)	15.0	7.9

* Vertical measurements of maximum depth. Values within parenthesis provide previously observed depths (from R.B. Langerhans) that differ from that observed here.

† Cave passages reach a known depth of 127 m.

(99 % purity). Since salinity varied with depth in the blue holes, we used five separate calibration curves for salinities 0, 5, 15, 25, and 35 ppt, where sample concentrations were determined using the calibration curve of the closest salinity. Due to calibration uncertainties, we only use Fe concentrations assessed using the Ferrozine method to compare relative concentrations between different layers within a given blue hole (Fig. 3). In all other instances, Fe concentrations obtained from ICP-OES (see below) were used for higher reliability.

H_2S was analyzed in the field immediately after sampling using a sulfide cuvette test (LCK 653, Hach, Loveland, CO, USA) on a portable spectrophotometer (DR Lange 1900; Hach, Loveland, CO, USA). Samples containing H_2S concentrations above the upper detection limit (2.0 mg L^{-1}) were diluted with Milli-Q water and immediately reanalyzed. Chlorophyll-*a* and phycocyanin were measured *in vivo* with a portable fluorometer (AquaFluor; Turner Designs, Sunnyvale, CA, USA). Samples for total organic carbon (TOC) analyses were acidified in the field with HCl (2M) and kept at 4 °C until analysis. On the day of sampling, color/absorbance (420 nm) was measured on filtered (GF/C Whatman; Maidstone, UK) water in a 1 cm cuvette. For pH measurements a 913 pH Meter (Metrohm, Herisau, Switzerland) was used. Samples for Fe, manganese (Mn), aluminum (Al), silica (Si) total phosphorus (TP), total nitrogen (TN), phosphate (PO_4^{3-}), nitrate (NO_3^-), and sulfate (SO_4^{2-}) were kept on ice until our return to the field station where they were stored frozen. TOC and TN concentrations were later analyzed in the lab with a TOC V-CPN analyzer (Shimadzu, Kyoto, Japan), using the non-purgeable organic matter method (NPOC). Fe, Mn, Al, Si and TP concentrations were analyzed with ICP-OES (Optima 8300; Perkin Elmer, Waltham, MA, USA), while SO_4^{2-}, NO_3^- and PO_4^{3-} concentrations were analyzed using Ion chromatography (816 Advanced Compact IC; Metrohm, Herisau, Switzerland). For metal analysis samples were acidified (1 % HNO_3) 24 hours prior to analysis.

Results

Water chemistry

The blue holes differed in morphological features and stratification patterns (Table 1). All of the examined blue holes, except Gollum, West Twin, and Murky Brown, were vertically stratified with fresh or brackish water overlying saline water (Fig. 3, Suppl. material S1). The depth of the freshwater layer in the stratified blue holes ranged from 2 m in Little Frenchman to over 30 m in Stalactite (Table 1). Oxic conditions with DO concentrations around 7 mg L^{-1} (lower for Little Frenchman) prevailed in the freshwater layer in all blue holes, while oxygen was absent in the saline layer in all of the deeper blue holes. Oxygen was present throughout the water column in two of the three blue holes without a saline layer (West Twin and Murky Brown), whereas the bottom water was anoxic in Gollum (Suppl. material S1). Temperature decreased with increasing depth in the freshwater layer, increased slightly in the halocline, and decreased again in the saline layer in stratified blue holes, ranging from 22.9 °C in the freshwater layer of Murky Brown to 30.1 °C in the halocline of Ken's blue hole (Fig. 3, Suppl. material S1).

Freshwater layer

Some of the studied blue holes had very clear water, such as Stalactite and Ken's with Secchi depths greater than 15 m and turbidity below 1 FTU, whereas others were comparatively turbid (e.g. Murky Brown with a Secchi depth below 2 m; Fig. 3, Suppl. material S1+S2). Unlike all other blue holes examined in this study, water color in Little Frenchman was brown, with TOC concentrations on average 4 times higher than in any other blue hole (> 20 mg L^{-1} compared to < 5.5 mg L^{-1} in the other blue holes; Fig. 3, Suppl. material S1+S2). Furthermore, Little Frenchman had the highest absorbance at 420 nm (7.5 m^{-1}), which was on average 9 times higher than in the other blue holes (from 0.4 m^{-1} in Cousteau's and Stalactite, to 2.8 m^{-1} in Hubcap; Suppl. material S2).

pH was similar between blue holes ranging from 7.6 to 8.6 in the freshwater layer (Suppl. material S2). The mean TP concentration was 16.1 ± 5.6 µg L^{-1} in the freshwater layer, while TN concentrations were more variable (mean 575 ± 428 µg L^{-1}; Fig. 3, Suppl. material S1+S2). NO_3^- concentrations ranged from below detection limit (< 15 µg L^{-1}) to 424 µg L^{-1} in the freshwater layers, while PO_4^{3-} was below detection limit (< 30 µg L^{-1}) throughout the water column in all blue holes (Suppl. material S2). SO_4^{2-} concentrations (31 ± 35 mg L^{-1}) were lowest in the freshwater layers and increased in the halocline as salinity increased, reaching the highest concentrations in the saline layer (Fig. 3, Suppl. material S2–S4). No H_2S was detected in any of the samples collected from the freshwater layer (Fig. 3, Suppl. Material S1). Si concentrations were lowest in the freshwater layer (0.35 ± 0.18 mg L^{-1}). Concentrations of other metals were low, below detection limit for Fe and Al, in all freshwater samples, while Mn concentrations were below 1 µg L^{-1} in the freshwater layer of all blue holes except for Little Frenchman where concentrations reached 3.5 µg L^{-1} (Fig. 3, Suppl. material S1+S2).

Halocline

A peak in turbidity, together with an increase in salinity and decline in DO compared to the freshwater layer, characterized the halocline in stratified blue holes. Overall, mean turbidity in the halocline was 7 times higher than in the freshwater layer with a maximum

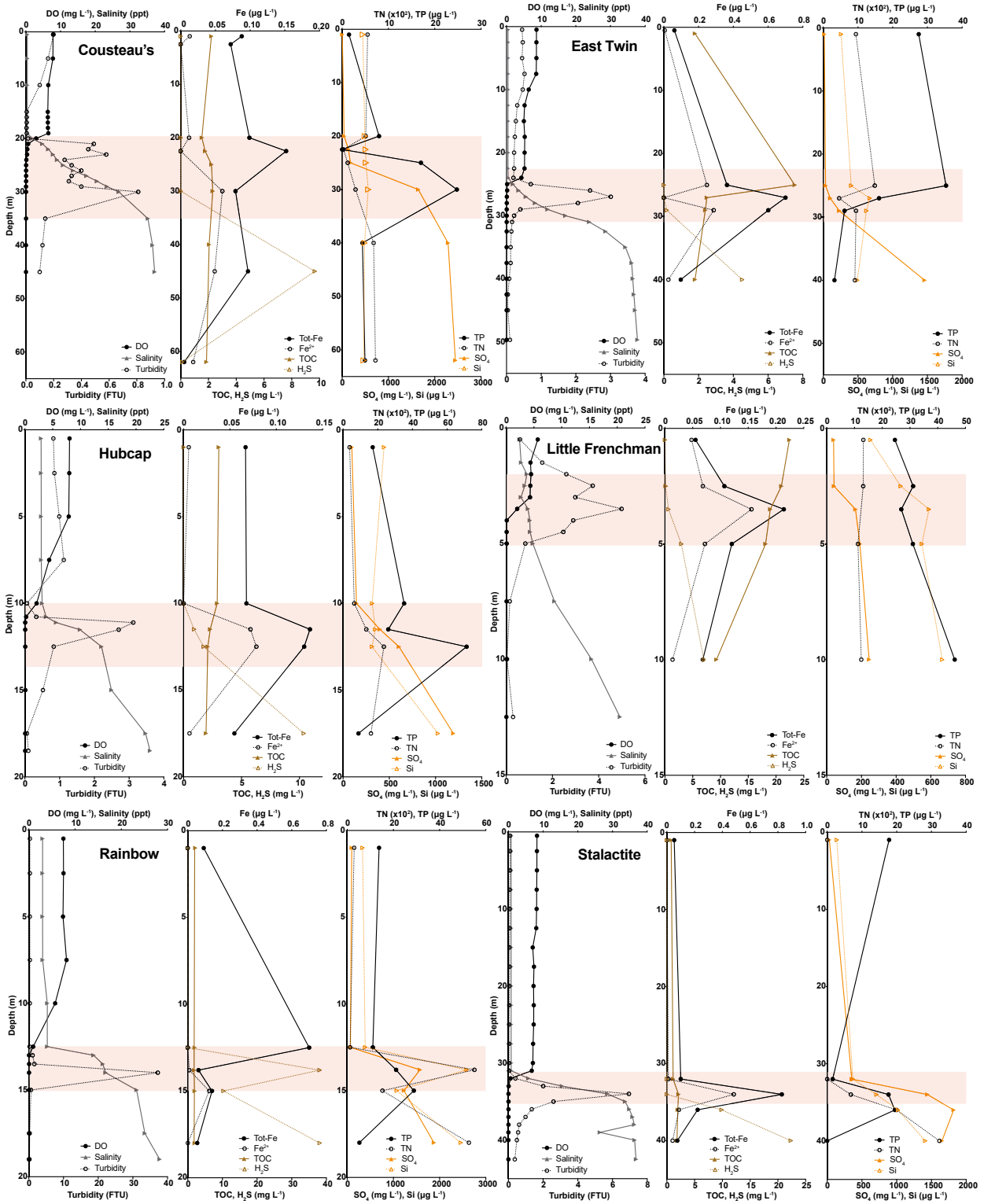

Fig. 3. Vertical profiles of dissolved oxygen (DO), salinity, turbidity, total iron (Tot-Fe), reduced iron (Fe^{2+}), total organic carbon (TOC), hydrogen sulfide (H_2S), total phosphorus (TP), total nitrogen (TN), sulfate (SO_4^{2-}), and silica (Si) concentration in six blue holes on Andros Island, The Bahamas. The shaded region denotes the halocline, i.e. a region of increasing salinity and turbidity accompanied by a reduction in DO.

turbidity of 126 FTU in the halocline of Ken's blue hole (Suppl. material S1). Mean TOC concentrations were higher in the halocline (5.4 ± 6.8 mg L^{-1}) compared to the other layers (Fig. 3, Suppl. material S1).

The presence of both H_2S and Fe^{2+} indicated that reducing conditions occurred in and below the halocline (Fig. 3, Suppl. material S1). Metal (Fe, Al and Mn) concentrations were low, and in many cases below detection limit, but Fe concentrations ranged from below 1 to 120 µg L^{-1} in the halocline, with the highest concentration found in Stalactite (Suppl. material S3). The overall mean Mn concentration for the haloclines was 21.9 ± 22.0 µg L^{-1}, while Al concentrations were below detection limit in all samples (Suppl. material S3). Average TP concentrations were 23.5 ± 16.6 µg L^{-1} in the halocline, which was higher than in the freshwater and saline layers (Fig. 3, Suppl. material S1+S3).

Saline layer

H_2S was detected in all stratified blue holes and concentrations reached maximum in the saline water where DO was absent and S available in high concentrations. H_2S concentrations ranged from 0.11 to 38.1 (mean 13.2 ± 12.9) mg L^{-1} in the saline layers (Fig. 3, Suppl. material S1+S4). The mean TN concentration was highest for the saline layer (mean 2.0 ± 1.6 mg L^{-1}), while NO_3^- concentrations on the other hand decreased with depth as oxygen got depleted (Fig. 3, Suppl. material S1+S4).

Table 2. Phytoplankton, zooplankton, and fish observed in the 10 sampled blue holes. For phytoplankton, only the dominant taxa are listed, while for zooplankton and fish all encountered species/taxa are listed. Higher taxonomical groups are presented where it was not possible to identify species.

Blue hole	Phytoplankton	Zooplankton	Fish
Cousteau's	*Coelosphaerium/Snowella**	Cyclopoid copepods	*Gambusia hubbsi*
	Planktolyngbya	Rotifers	*Gobiomorus dormitor*
	Naiadinium polonicum		
East Twin	*Coelosphaerium/Snowella**	Calanoid copepods	*Gambusia hubbsi*
	Planktolyngbya	Cyclopoid copepods	*Lophogobius cyprinoides*
	Naiadinium polonicum	Rotifers	
Gollum	*Coelosphaerium/Snowella**	Calanoid copepods	*Gambusia hubbsi*
	Naiadinium polonicum	Cyclopoid copepods	*Cyprinodon variegatus*
Hubcap	*Coelosphaerium/Snowella**	Calanoid copepods	*Gambusia hubbsi*
	Planktolyngbya	Cyclopoid copepods	*Cyprinodon variegatus*
	Naiadinium polonicum	Rotifers	
	Small thecate dinoflagellate		
Ken's	NA	Calanoid copepods	*Gambusia hubbsi*
		Cyclopoid copepods	*Cyprinodon variegatus*
			Lophogobius cyprinoides
Little Frenchman	*Planktolyngbya*	Calanoid copepods	*Gambusia hubbsi*
	Large thecate dinoflagellate		
	Small thecate dinoflagellate		
Murky Brown	*Planktolyngbya*	Calanoid copepods	*Gambusia hubbsi*
	Pseudanabaena		*Gobiomorus dormitor*
	Naiadinium polonicum		
Rainbow	*Coelosphaerium/Snowella**	Calanoid copepods	*Gambusi hubbsi*
	Small thecate dinoflagellate	Cyclopoid copepods	*Cyprinodon variegatus*
		Rotifers	
Stalactite	*Picocyanobacteria*	Calanoid copepods	*Gambusia hubbsi*
	Large thecate dinoflagellate	Cyclopoid copepods	*Gobiomorus dormitor*
	Small thecate dinoflagellate	Rotifers	
West Twin	*Coelosphaerium/Snowella*	Calanoid copepods	*Gambusia hubbsi*
	Planktolyngbya	Cyclopoid copepods	*Gobiomorus dormitor*
		Rotifers	

* The taxon listed as *Coelosphaerium/Snowella* denotes that this species was likely either a *Snowella* or *Coelosphaerium* sp.

Biology

The phytoplankton community (>10 µm fraction) consisted of a limited number of taxa that occurred in most of the blue holes, but in different proportions (Table 2). Dominant taxa were either cyanobacteria (colonial or filamentous) or dinoflagellates. The dinoflagellate *Naiadinium polonicum*, was encountered in large numbers in Cousteau's, East Twin, Gollum, Hubcap and Murky Brown (Table 2). Phytoplankton biomass, determined by chlorophyll-*a*, was very low (<1 µg chl-*a* L^{-1}) in most blue holes. The exceptions were Little Frenchman and Murky Brown, both of which had high turbidity and high abundances of filamentous cyanobacteria and dinoflagellates.

The zooplankton community was similarly limited in taxa with calanoid and/or cyclopoid copepods being present in all blue holes, as well as rotifers (*Keratella* spp.) being observed in many (Table 2). The small livebearing Bahamas mosquitofish (*Gambusia hubbsi*), was also present in all blue holes, while other small fish species (*Cyprinodon variegatus, Lophogobius cyprinoides*) were only occasionally present (Table 2). Cousteau's, Murky Brown, Stalactite and West Twin also had the piscivorous bigmouth sleeper (*Gobiomorus dormitor*) (Table 2).

Discussion

Inland blue holes are rare and unique ecosystems since they contain a freshwater upper part and a deeper part influenced by marine water and anoxic conditions. Our current understanding of the water chemistry at the interface between the freshwater and saline layer of blue holes is poor. This, together with the lacking description of biota in these isolated ecosystems constitutes the rationale for our broad study on a large set of blue holes.

As expected, the majority of the studied blue holes here were vertically stratified with freshwater overlying saline anoxic water. With relatively stable oxygen and salinity gradients, these aquatic systems are great settings for biogeochemical studies. While blue holes varied considerably in transparency and depth of freshwater layer, they exhibited relatively little variation in for instance pH and TP concentrations. Moreover, TOC concentrations for all blue holes, except for Little Frenchman, were in the same range as the dissolved organic carbon (DOC) concentrations found in Magical blue hole on Abaco Island, The Bahamas (<4 mg L^{-1}; Haas et al. 2018). The notably higher TOC concentrations in Little Frenchman were most likely caused by the presence of mangroves in this blue hole, as mangroves did not occur in any other blue hole examined in this study. Mangroves can represent a major source of organic carbon to the open ocean, even though they cover only a minor fraction of the landmasses globally (Dittmar et al. 2006), and have been identified as an important player in the global carbon cycle (Maher et al. 2013).

Nutrient (N and P) concentrations in the Andros blue holes were in the range of what has previously been reported for coastal and inland aquatic systems in the Bahama Archipelago (Koch & Madden 2001; Paerl et al. 2003; Lapointe et al. 2004; Haas et al. 2018). TP concentrations varied strongly with depth, peaking in the halocline where particulate P could be present either as part of inorganic minerals, or in organic matter suspended at the density gradient. A major source of N in inland blue holes is presumably wet deposition, as atmospheric loadings from southeastern USA have been reported to provide Abaco Island (northeast of Andros), with significant amounts of N (Barile & Lapointe 2005). Furthermore, fixation of atmospheric N_2 by cyanobacteria – providing a source of N for carbonate producers and others – has been suggested to support productivity in the otherwise nutrient poor environments of The Bahamas (Swart et al. 2014).

The halocline had dramatically higher turbidity relative to the rest of the water column in all blue holes with a saline sublayer. This likely reflects a combination of inorganic and organic particles originating from the freshwater layer that are suspended in the halocline as a result of the density gradient between the fresh and saline water (Gonzalez et al. 2011). The presence of both H_2S and Fe^{2+} indicates reducing conditions in and below the halocline. Furthermore, the declining NO_3^- concentration with depth suggests NO_3^- reduction at lower oxygen concentrations. This notion is strengthened by previous studies where dissolved inorganic N was found to be present below the halo-chemocline in blue holes in the form of ammonium (NH_4^+), and above the halo-chemocline in the form of NO_3^- (Lapointe et al. 2004; Haas et al. 2018). Although we did not measure NH_4^+, the decline in NO_3^- indicates N reduction and occurrence of N as NH_4^+ in sub-oxic waters.

We found H_2S in all stratified blue holes and the H_2S concentrations reached a maximum in the saline, anoxic layers with high S concentrations. H_2S is a product of bacterially mediated SO_4^{2-} reduction, which has previously been shown to occur under reducing conditions in blue holes (Bottrell et al. 1991; Gonzalez et al. 2011; Haas et al. 2018). H_2S concentrations in the

halocline were in the same range as found by Gonzales et al. (2011), and generally higher than concentrations reported by Haas et al. (2018), measured in two blue holes on Abaco Island. The fact that total Fe and Fe^{2+} concentrations peaked in the halocline, while the H_2S concentrations reached their maximum in the saline layer for most of the stratified blue holes, could be due to more SO_4^{2-} being present in the saline water and because Fe reduction occurs at a higher redox potential than sulfate reduction. Furthermore, H_2S may react with Fe^{2+} forming stable and insoluble Fe sulfides (FeS – FeS_2) (Engstrom & Wright 1984). Pyrite (FeS_2) formation has been suggested to occur in the halocline close to the walls of the blue holes where pH is buffered by calcite dissolution (Bottrell et al. 1991), and more recently in blue hole microbial mats that may trap H_2S and Fe (Haas et al. 2018). Low Fe concentrations observed throughout the water column of the blue holes are however most likely a result of the Fe poor carbonate bedrock. The main source of Fe in The Bahamas is from atmospherically deposited Sahara sand (Mahowald et al. 2005; Swart et al. 2014; Haas et al. 2018), and the deposition of Fe containing dust has varied during climate fluctuations (Swart et al. 2010). Red dust layers filling cavities in blue holes have been observed by cave divers and settling of Fe reducing bacteria on such Fe dust features have been suggested to have initialized formations of microbial mats rich in Fe (Haas et al. 2018).

The halocline has been described as a microbial hotspot dominated by anoxygenic phototrophic bacteria, while SO_4^{2-} reducing bacteria have also been found in saline anoxic waters of blue holes (Gonzalez et al. 2011). The microbially active layer between the fresh and saline water is supported by surface-derived organic matter getting trapped in the density gradient between fresh and saline water. Microbes in anchialine systems obtain energy from reduced compounds produced during organic matter degradation (Pohlman 2011), and it has been shown that SO_4^{2-} reducers and other heterotrophs abundant in the microbial mats in blue holes on Abaco Island are limited by organic carbon availability (Haas et al. 2018). Although TOC concentrations were not elevated in the halocline in this study, the amount of DNA extracted from water sample filtrates (on polyethersulfone membrane filters with a pore size of 0.2 µm) was 10-fold higher in the halocline than in the freshwater and deeper saline water (unpublished data). Both SO_4^{2-} reducing and S^{2-} oxidizing bacteria (Gonzalez et al. 2011), were abundant in the halocline (as determined through DNA barcoding; unpublished data).

Overall, the phytoplankton species richness was very low and in most blue holes studied only 3–4 taxa were encountered (Table 2), most of which were present in multiple blue holes. Occasional specimens of other taxa were sometimes detected, but the abundance of these was extremely low. Dominant taxa in each blue hole belonged either to cyanobacteria or Dinophyceae. While the cyanobacteria observed were either semi-spherical colonies or filaments, the dinoflagellates were large, flagellated, unicellular species. Both occupy a similar niche, but with quite different adaptive strategies to stay suspended. While dinoflagellates efficiently regulate their position in the water by swimming with their flagella, the cyanobacteria are dependent on high buoyancy due to colony shape, mucilage and gas vesicles (Reynolds 2006). Taxa with high sinking rates, such as diatoms, were rare in the blue holes. While cyanobacteria and dinoflagellates are usually found in meso- to eutrophic conditions, they are also well adapted to lakes with high column stability, and non-turbulent conditions (Smayda & Reynolds 2003), as found in these inland blue holes.

Interestingly, only *Naiadinium polonicum* was present in a wide range of surface water salinities (0.22–3.0 ppt), but rarely coexisted with other thecate dinoflagellates, which only occurred in blue holes where surface water was brackish (0.8–3.3 ppt). This suggests that *N. polonicum*, a species that is also known to be potentially ichthyotoxic (Roset et al. 2002), might be the only truly freshwater adapted dinoflagellate species in these blue holes, while the other dinoflagellates may have a marine origin and are unable to survive and propagate in freshwater. Previous studies on dinoflagellate salinity tolerance in Antarctic lakes suggest that marine-derived dinoflagellates have adapted to both brackish and hypersaline lakes, but do not grow in freshwater lakes (Rengefors et al. 2012; Rengefors et al. 2015).

The diversity of zooplankton was also limited, with only a small number of taxa present in nearly all the blue holes investigated. Copepods were most abundant of the primary consumer level in these systems, although rotifers, such as *Keratella* spp. were also present in most blue holes. Notably, the third major group of freshwater zooplankton, cladocerans (e.g. *Daphnia*) were absent from the investigated blue holes, even though cladocerans have been documented in The Bahamas previously (Collado et al. 1984). Since all sampled blue holes contained vertebrate predators, predation is potentially contributing to the apparent absence of cladocerans in these systems. For instance, due to their larger size in comparison to rotifers, cladocerans

may be more susceptible to predation according to the size efficiency hypothesis (Brooks & Dodson 1965). Experimental studies have also shown that *Gambusia holbrooki*, a mosquitofish species closely related to the Bahamas mosquitofish *G. hubbsi*, does selectively predate upon cladocerans (Blanco, Romo, & Villena 2004). Furthermore, nutrient availability may influence zooplankton community composition among blue holes. While the only two blue holes where cyclopoid copepods were absent had narrow, relatively turbid freshwater layers with high TN concentrations (Little Frenchman, Murky Brown), the only blue hole without calanoid copepods (Cousteau's) had the lowest surface TP concentration.

The Bahamas mosquitofish (*Gambusia hubbsi*) was present in all investigated blue holes, and coexisted with one or two other small planktivorous/invertivorous fish species in some blue holes. A major difference in the fish community across the investigated blue holes was the presence/absence of the piscivorous bigmouth sleeper (*Gobiomorus dormitor*), which has an effect on the behavior of other biota e.g. zooplankton (Sha et al. 2020). As predation can shape community structure, trophic dynamics and the adaptive landscape of resident organisms in aquatic systems, the presence of a top predator likely has far-reaching impact on biodiversity and species interactions in the blue holes (Langerhans et al. 2007; Heinen et al. 2013; Martin, McGee, & Langerhans 2015; Langerhans 2017). Previous work has documented that most inland blue holes on Andros have relatively simple fish assemblages, with the number of species largely corresponding to the theory of island biogeography predicting more species being present in blue holes with a larger surface diameter and situated closer to possible sources of colonization, but not in deeper blue holes (Langerhans & Gifford 2009).

Conclusions

The between-site similarity of inland blue holes on Andros Island contrasts with the great variability in water chemistry and biota typically found among lakes in temperate regions. Although there were differences in the freshwater layers between blue holes, this did not seem to be affected by their depth or the water chemistry below the halocline. Despite the low biodiversity in all blue holes, there were differences in species composition, likely dependent on differences in water chemistry and predation regimes. These salinity stratified systems exhibited a great change in water chemistry when reaching the halocline, where the gradual loss of oxygen facilitates the reduction of redox sensitive elements such as N, Fe and S. Although data from this study only represents a snapshot of the water chemistry and biota, comparisons with previous studies suggest that the seasonal and between-year variability in inland blue holes is minor (Heinen et al. 2013). Hence, the data presented here reinforce that inland blue holes are highly interesting for biogeochemical research, and can be used in experimental evolution field studies as they provide natural replicates for scientific inquiry. Moreover, the relatively simple plankton and fish communities offer excellent potential to study food-web interactions and population genetics.

Acknowledgements

We thank the Helge Ax:son Johnsons foundation, The Royal Physiographic Society, and County Governor Per Westling Memorial Fund for financial support. We thank prof. Øjvind Moetrup, Copenhagen University, for identifying *Naiadinium polonicum* by scanning electron microscopy. Thanks to Sofia Mebrahtu Wisén at the Instrumental Chemistry Facility, Department of Biology, Lund University, for inorganic analyses. We are also grateful to The Bahamas government for permission to conduct the fieldwork and to Wilfred Johnson for support in the field.

Authors' contributions

C.B., M.Š., R.G. and S.D.H. conceived and led the study. C.B., M.Š., R.G. and S.D.H. conducted the analyses. C.B. wrote the first version with substantial contributions from M.Š., R.G., S.D.H., M.L., L-A.H., R.B.L., Ch.B. and K.R. All authors aided in fieldwork and provided valuable guidance both during the research process and the revision of the manuscript.

References

Barile, P. J., & Lapointe, B. E. (2005). Atmospheric nitrogen deposition from a remote source enriches macroalgae in coral reef ecosystems near Green Turtle Cay, Abacos, Bahamas. *Marine Pollution Bulletin, 50*(11), 1262–1272. https://doi.org/10.1016/j.marpolbul.2005.04.031 PMID:15913662

Blanco, S., Romo, S., & Villena, M. J. (2004). Experimental study on the diet of mosquitofish (Gambusia holbrooki) under different ecological conditions in a shallow lake. *International Review of Hydrobiology, 89*(3), 250–262. https://doi.org/10.1002/iroh.200310684

Bottrell, S. H., Smart, P. L., Whitaker, F., & Raiswell, R. (1991). Geochemistry and isotope systematics of sulfur in the mixing zone of Bahamian blue holes. *Applied Geochemistry, 6*(1), 97–103. https://doi.org/10.1016/0883-2927(91)90066-X

Brooks, J. L., & Dodson, S. I. (1965). Predation body size and composition of plankton. *Science, 150*(3692), 28–35. https://doi.org/10.1126/science.150.3692.28

Buchan, K. C. (2000). The Bahamas. *Marine Pollution Bulletin, 41*(1–6), 94–111. https://doi.org/10.1016/S0025-326X(00)00104-1

Collado, C., Fernando, C. H., & Sephton, D. (1984). *The freshwater zooplankton of Central America and the Caribbean*. In H. J. Dumont, & J. G. Tundisi (Eds.), Tropical Zooplankton. Developments in Hydrobiology, vol 23. Dordrecht: Springer. https://doi.org/10.1007/978-94-017-3612-1_8

Dittmar, T., Hertkorn, N., Kattner, G., & Lara, R. J. (2006). Mangroves, a major source of dissolved organic carbon to the oceans. *Global Biogeochemical Cycles, 20*(1), n/a. https://doi.org/10.1029/2005GB002570

Engstrom, D. R., & Wright, H. E. J. (1984). Chemical stratigraphy of lake sediments as a record of environmental change. In E. Y. Haworth & J. W. G. Lund (Eds.), *Lake sediments and environmental history* (pp. 11–68). Leicester: Leicester University Press.

Fairbanks, R. G. (1989). A 17,000-year glacio-eustatic sea-level record – influence of glacial melting rates on the younger Dryas event and deep-ocean circulation. *Nature, 342*(6250), 637–642. https://doi.org/10.1038/342637a0

Fukushima, T., Matsushita, B., Subehi, L., Setiawan, F., & Wibowo, H. (2017). Will hypolimnetic waters become anoxic in all deep tropical lakes? *Scientific Reports, 7*(1), 45320. https://doi.org/10.1038/srep45320

Garman, K. M., & Garey, J. R. (2005). The transition of a freshwater karst aquifer to an anoxic marine system. *Estuaries, 28*(5), 686–693. https://doi.org/10.1007/BF02732907

Gonzalez, B. C., Iliffe, T. M., Macalady, J. L., Schaperdoth, I., & Kakuk, B. (2011). Microbial hotspots in anchialine blue holes: Initial discoveries from the Bahamas. *Hydrobiologia, 677*(1), 149–156. https://doi.org/10.1007/s10750-011-0932-9

Haas, S., de Beer, D., Klatt, J. M., Fink, A., Rench, R. M., Hamilton, T. L., . . . Macalady, J. L. (2018). Low-Light Anoxygenic Photosynthesis and Fe-S-Biogeochemistry in a Microbial Mat. *Frontiers in Microbiology, 9*, 858. https://doi.org/10.3389/fmicb.2018.00858 PMID:29755448

Hastings, A. K., Krigbaum, J., Steadman, D. W., & Albury, N. A. (2014). Domination by Reptiles in a Terrestrial Food Web of the Bahamas Prior to Human Occupation. *Journal of Herpetology, 48*(3), 380–388. https://doi.org/10.1670/13-091R1

Heinen, J. L., Coco, M. W., Marcuard, M. S., White, D. N., Peterson, M. N., Martin, R. A., & Langerhans, R. B. (2013). Environmental drivers of demographics, habitat use, and behavior during a post-Pleistocene radiation of Bahamas mosquitofish (Gambusia hubbsi). *Evolutionary Ecology, 27*(5), 971–991. https://doi.org/10.1007/s10682-012-9627-6

Iliffe, T. M., & Kornicker, L. S. (2009). Worldwide diving discoveries of living fossil animals from the depths of anchialine and marine caves. *Smithsonian Contributions to the Marine Sciences,* 38, 269–280.

Koch, M. S., & Madden, C. J. (2001). Patterns of primary production and nutrient availability in a Bahamas lagoon with fringing mangroves. *Marine Ecology Progress Series, 219*, 109–119. https://doi.org/10.3354/meps219109

Kovacs, S. E., van Hengstum, P. J., Reinhardt, E. G., Donnelly, J. P., & Albury, N. A. (2013). Late Holocene sedimentation and hydrologic development in a shallow coastal sinkhole on Great Abaco Island, The Bahamas. *Quaternary International, 317*, 118–132. https://doi.org/10.1016/j.quaint.2013.09.032

Langerhans, R. B. (2009). Morphology, performance, fitness: Functional insight into a post-Pleistocene radiation of mosquitofish. *Biology Letters, 5*(4), 488–491. https://doi.org/10.1098/rsbl.2009.0179 PMID:19411270

Langerhans, R. B. (2017). Predictability and parallelism of multitrait adaptation. *The Journal of Heredity, 109*(1), 59–70. https://doi.org/10.1093/jhered/esx043 PMID:28482006

Langerhans, R. B., & Gifford, M. E. (2009). Divergent selection, not life-history plasticity via food limitation, drives morphological divergence between predator regimes in *Gambusia hubbsi*. *Evolution, 63*(2), 561–567. https://doi.org/10.1111/j.1558-5646.2008.00556.x PMID:19154366

Langerhans, R. B., Gifford, M. E., & Joseph, E. O. (2007). Ecological speciation in Gambusia fishes. *Evolution; International Journal of Organic Evolution, 61*(9), 2056–2074. https://doi.org/10.1111/j.1558-5646.2007.00171.x PMID:17767582

Lapointe, B. E., Barile, P. J., Yentsch, C. S., Littler, M. M., Littler, D. S., & Kakuk, B. (2004). The relative importance of nutrient enrichment and herbivory on macroalgal communities near Norman's Pond Cay, Exumas Cays, Bahamas: A "natural" enrichment experiment. *Journal of Experimental Marine Biology and Ecology, 298*(2), 275–301. https://doi.org/10.1016/S0022-0981(03)00363-0

Lee, M., Zhang, H., Sha, Y., Hegg, A., Ugge, G. E., Vinterstare, J., . . . Hansson, L. A. (2019). Low-latitude zooplankton pigmentation plasticity in response to multiple threats. *Royal Society Open Science, 6*(7), 190321. https://doi.org/10.1098/rsos.190321 PMID:31417735

Maher, D. T., Santos, I. R., Golsby-Smith, L., Gleeson, J., & Eyre, B. D. (2013). Groundwater-derived dissolved inorganic and organic carbon exports from a mangrove tidal creek: The missing mangrove carbon sink? *Limnology and Oceanography, 58*(2), 475–488. https://doi.org/10.4319/lo.2013.58.2.0475

Mahowald, N. M., Baker, A. R., Bergametti, G., Brooks, N., Duce, R. A., Jickells, T. D., . . . Tegen, I. (2005). Atmospheric global dust cycle and iron inputs to the ocean. *Global Biogeochemical Cycles, 19*(4), n/a. https://doi.org/10.1029/2004GB002402

Martin, R. A., McGee, M. D., & Langerhans, R. B. (2015). Predicting ecological and phenotypic differentiation in the wild: A case of piscivorous fish in a fishless environment. *Biological Journal of the Linnean Society. Linnean Society of London, 114*(3), 588–607. https://doi.org/10.1111/bij.12449

Mylroie, J. E., & Carew, J. L. (1995). Geology and karst geomorphology of San-Salvador Island, Bahamas. *Carbonates and Evaporites, 10*(2), 193–206. https://doi.org/10.1007/BF03175404

Mylroie, J. E., Carew, J. L., & Moore, A. I. (1995). Blue holes: Definition and genesis. *Carbonates and Evaporites, 10*(2), 225–233. https://doi.org/10.1007/BF03175407

Mylroie, J. E., & Mylroie, J. R. (2013). Caves and karst of the Bahama Islands. In M. J. Lace, & J. E. Mylroie (Eds.), *Coastal karst landforms. Coastal Research Library, vol 5* (pp. 147–176) Dordrecht: Springer. https://doi.org/10.1007/978-94-007-5016-6_7

Paerl, H. W., Steppe, T. F., Buchan, K. C., & Potts, M. (2003). Hypersaline cyanobacterial mats as indicators of elevated tropical hurricane activity and associated climate change. *Ambio, 32*(2), 87–90. https://doi.org/10.1579/0044-7447-32.2.87 PMID:12733791

Pohlman, J. W. (2011). The biogeochemistry of anchialine caves: Progress and possibilities. *Hydrobiologia, 677*(1), 33–51. https://doi.org/10.1007/s10750-011-0624-5

Rengefors, K., Logares, R., & Laybourn-Parry, J. (2012). Polar lakes may act as ecological islands to aquatic protists. *Molecular Ecology, 21*(13), 3200–3209. https://doi.org/10.1111/j.1365-294X.2012.05596.x PMID:22564188

Rengefors, K., Logares, R., Laybourn-Parry, J., & Gast, R. J. (2015). Evidence of concurrent local adaptation and high phenotypic plasticity in a polar microeukaryote. *Environmental Microbiology, 17*(5), 1510–1519. https://doi.org/10.1111/1462-2920.12571 PMID:25041758

Reynolds, C. S. (2006). *The ecology of phytoplankton*. Cambridge: Cambridge University Press. https://doi.org/10.1017/CBO9780511542145

Roset, J., Gibello, A., Aguayo, S., Dominguez, L., Alvarez, M., Fernandez-Garayzabal, J. F., . . . Munoz, M. J. (2002). Mortality of rainbow trout Oncorynchus mykiss (Walbaum) associated with freshwater dinoflagellate bloom Peridinium polonicum (Woloszynska) in a fish farm. *Aquaculture Research, 33*(2), 141–145. https://doi.org/10.1046/j.1365-2109.2002.00660.x

Sha, Y., Zhang, H., Lee, M., Björnerås, C., Škerlep, M., Gollnisch, R., . . . Hansson, L.-A. (2020). Diel vertical migration of copepods and its environmental drivers in subtropical Bahamian blue holes. Aquatic Ecology. https://doi.org/10.1007/s10452-020-09807-4

Smayda, T. J., & Reynolds, C. S. (2003). Strategies of marine dinoflagellate survival and some rules of assembly. *Journal of Sea Research, 49*(2), 95–106. https://doi.org/10.1016/S1385-1101(02)00219-8

Smith, I. K., & Vankat, J. L. (1992). Dry evergreen forest (coppice) communities of north Andros Island, Bahamas. *Bulletin of the Torrey Botanical Club, 119*(2), 181–191. https://doi.org/10.2307/2997030

Steadman, D. W., Albury, N. A., Kakuk, B., Mead, J. I., Soto-Centeno, J. A., Singleton, H. M., & Franklin, J. (2015). Vertebrate community on an ice-age Caribbean island. *Proceedings of the National Academy of Sciences of the United States of America, 112*(44), E5963–E5971. https://doi.org/10.1073/pnas.1516490112 PMID:26483484

Steadman, D. W., Franz, R., Morgan, G. S., Albury, N. A., Kakuk, B., Broad, K., . . . Dilcher, D. L. (2007). Exceptionally well preserved late Quaternary plant and vertebrate fossils from a blue hole on Abaco, The Bahamas. *Proceedings of the National Academy of Sciences of the United States of America, 104*(50), 19897–19902. https://doi.org/10.1073/pnas.0709572104 PMID:18077421

Stookey, L. L. (1970). Ferrozine – a new spectrophotometric reagent for iron. *Analytical Chemistry, 42*(7), 779–781 https://doi.org/10.1021/ac60289a016

Swart, P. K., Arienzo, M., Broad, K., Clement, A., & Kakuk, B. (2010). Blue Holes in Bahamas: Repositories of Climate, Anthropogenic, and Archaeological Changes over the Past 300 000 Years. *Journal of Earth Science, 21*(S1), 265. https://doi.org/10.1007/s12583-010-0231-9

Swart, P. K., Oehlert, A. M., Mackenzie, G. J., Eberli, G. P., & Reijmer, J. J. G. (2014). The fertilization of the Bahamas by Saharan dust: A trigger for carbonate precipitation? *Geology, 42*(8), 671–674. https://doi.org/10.1130/G35744.1

Viollier, E., Inglett, P. W., Hunter, K., Roychoudhury, A. N., & Van Cappellen, P. (2000). The ferrozine method revisited: Fe(II)/Fe(III) determination in natural waters. *Applied Geochemistry, 15*(6), 785–790. https://doi.org/10.1016/S0883-2927(99)00097-9

Whitaker, F. F., & Smart, P. L. (1997). Groundwater circulation and geochemistry of a karstified bank-marginal fracture system, South Andros Island, Bahamas. *Journal of Hydrology (Amsterdam), 197*(1–4), 293–315. https://doi.org/10.1016/S0022-1694(96)03274-X

Manuscript received: 21 April 2020
Revisions requested: 20 July 2020
Revised version received: 12 September 2020
Manuscript accepted: 14 September 2020

The pdf version of this paper includes an electronic supplement

Please save the electronic supplement contained in this pdf-file by clicking the blue frame above. After saving rename the file extension to .zip (for security reasons Adobe does not allow to embed .exe, .zip, .rar etc. files).

Table of contents – Electronic Supplementary Material (ESM)

Type of supporting information	Description
S1	Vertical profiles of dissolved oxygen (DO), salinity, turbidity, total iron (Tot-Fe), reduced iron (Fe^{2+}), total organic carbon (TOC), hydrogen sulfide (H_2S), total phosphorus (TP), total nitrogen (TN), sulfate (SO_4^{2-}), and silica (Si) concentration in four blue holes on Andros Island, The Bahamas.
S2	Summary of the physicochemical variables measured in the freshwater layer of the blue holes.
S3	Summary of the physicochemical variables measured in the halocline of the blue holes.
S4	Summary of the physicochemical variables measured in the saline layer of the blue holes.

SUPPLEMENTARY MATERIAL

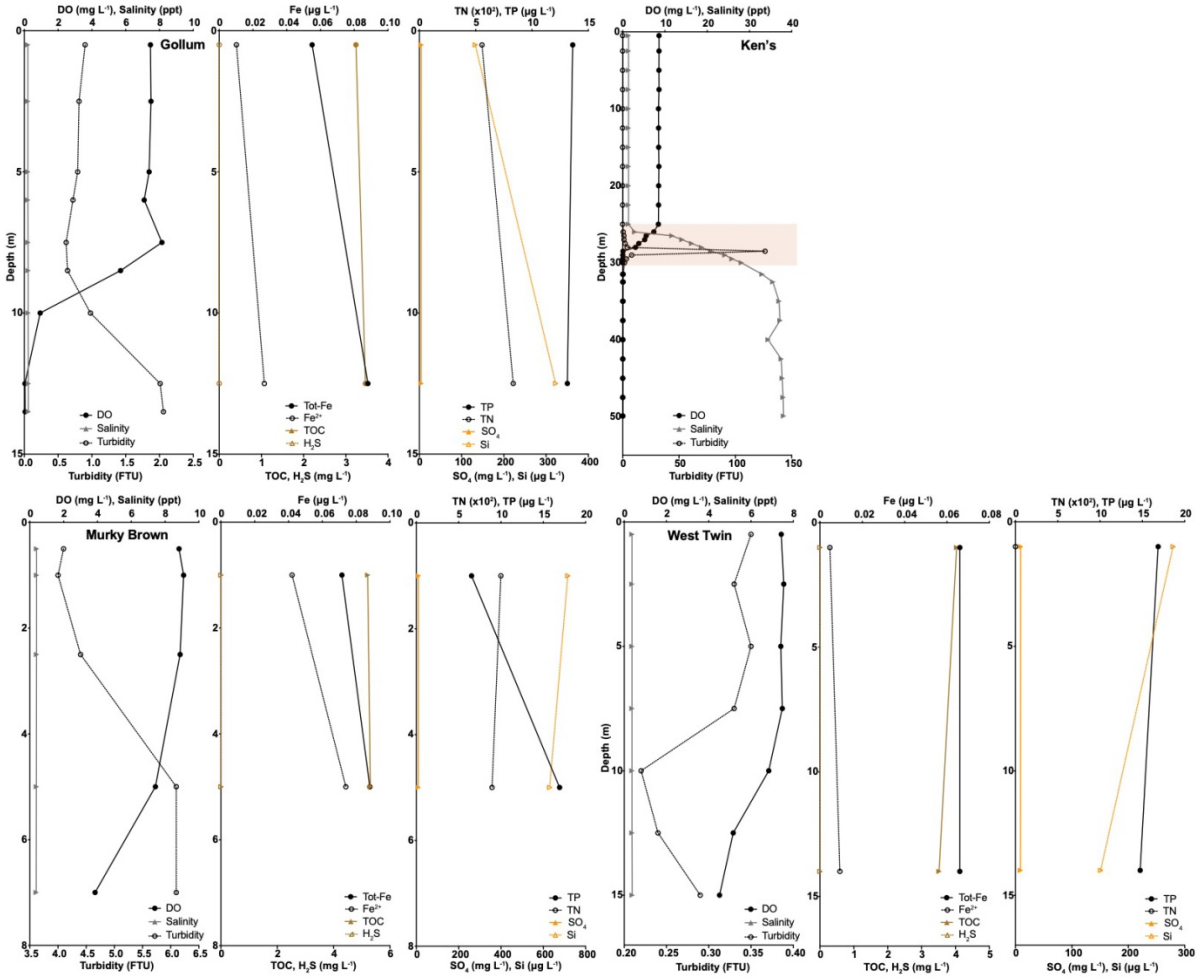

S1. Vertical profiles of dissolved oxygen (DO), salinity, turbidity, total iron (Tot-Fe), reduced iron (Fe^{2+}), total organic carbon (TOC), hydrogen sulfide (H_2S), total phosphorus (TP), total nitrogen (TN), sulfate (SO_4^{2-}), and silica (Si) concentration in four blue holes on Andros Island, The Bahamas. For the stratified blue hole (Ken's), the shaded region denotes the halocline, i.e. a region of increasing salinity and turbidity accompanied by a reduction in DO.

S2. Summary of the physicochemical variables measured in the freshwater layer of the blue holes. Top row in each cell show means with standard deviations within parenthesis, and the row below shows medians and ranges (min – max).

Variable	Cousteau's	East Twin	Gollum	Hubcap	Ken's	Little Frenchman	Murky Brown	Rainbow	Stalactite	West Twin
DO (mg L^{-1})	6.8 (0.66) 6.4 (6.3 - 7.8)	6.5 (1.8) -	4.9 (3.5) 7.1 (0.04 - 8.2)	6.1 (2.7) 7.9 (2.1 - 8.0)	8.5 (0.05) 8.5 (8.5 - 8.6)	5.0 (0.92) 5.0 (4.4 - 5.7)	7.6 (2.2) 8.8 (3.9 - 9.1)	6.2 (2.7) 7.4 (0.94 - 8.2)	7.6 (0.55) 7.3 (6.8 - 8.2)	6.6 (1.3) 7.4 (4.5 - 7.6)
Salinity (ppt)	0.42 (0.01) 0.42 (0.42 - 0.43)	0.43 (0.02) -	0.22 (0.01) 0.22 (0.21 - 0.24)	3.0 (0.08) 2.9 (2.9 - 3.1)	1.4 (0) 1.4 (1.4 - 1.4)	2.6 (0.21) 2.6 (2.4 - 2.7)	0.39 (0.01) 0.40 (0.38 - 0.40)	3.3 (0.53) 3.0 (3.0 - 4.0)	0.80 (0.01) 0.80 (0.79 - 0.81)	0.37 (0.01) 0.37 (0.37 - 0.38)
Turbidity (FTU)	0.06 (0.08) 0.01 (0.01 - 0.20)	0.35 (0.12) -	1.1 (0.57) 0.81 (0.62 - 2.1)	0.77 (0.41) 0.85 (0.06 - 1.1)	0.06 (0.01) 0.06 (0.05 - 0.06)	1.1 (0.68) 1.1 (0.60 - 1.6)	4.9 (1.1) 4.4 (4.0 - 6.1)	0.29 (0.03) 0.30 (0.22 - 0.31)	0.07 (0.02) 0.07 (0.04 - 0.10)	0.30 (0.05) 0.33 (0.22 - 0.35)
Temperature (°C)	24.6 (0.8) 24.1 (24.0 - 26.0)	25.0 (0.9) -	24.2 (0.8) 23.9 (23.4 - 25.3)	24.6 (1.4) 24.1 (23.3 - 26.1)	25.4 (0.1) 25.3 (25.3 - 25.5)	23.9 (0.4) 23.9 (23.7 - 24.2)	25.2 (2.1) 25.9 (22.9 - 27.4)	24.8 (1.2) 25.0 (23.3 - 25.8)	25.2 (0.5) 25.1 (24.6 - 26.2)	23.9 (0.8) 24.4 (23.0 - 24.6)
pH	8.0 (7.60 - 8.36)	8.4*	8.0 (7.7 - 8.3)	8.0 (7.8 - 8.3)	-	8.0*	8.5 (8.4 - 8.6)	8.4 (8.3 - 8.4)	8.3*	8.3 (8.2 - 8.4)
Chl a (µg L^{-1})	0.57 (0.32) 0.57 (0.35 - 0.80)	0.16* -	0.61 (0.40) 0.61 (0.32 - 0.90)	0.66 (0.14) 0.66 (0.57 - 0.76)	- -	8.6* -	1.8 (0.90) 1.8 (1.2 - 2.5)	0.23 (0.07) 0.23 (0.19 - 0.28)	- -	0.04 (0.06) 0.04 (0 - 0.08)
Phycocyanin (µg L^{-1})	8.8 (0.29) 8.8 (8.6 - 9.0)	4.5* -	15 (13) 15 (6.2 - 25)	4.2 (3.5) 4.2 (1.7 - 6.6)	- -	21* -	17 (12) 17 (8.9 - 25)	2.6 (0.7) 2.6 (2.1 - 3.1)	1.3* -	8.5 (0.45) 8.5 (8.2 - 8.8)
TOC (mg L^{-1})	2.2* -	1.8* -	3.4 (0.16) 3.4 (3.2 - 3.5)	4.0 (0.10) 3.0 (2.9 - 3.0)	- -	22.4* -	5.3 (0.10) 5.3 (5.2 - 5.3)	1.9 (0.10) 1.9 (1.9 - 2.0)	0.78* -	3.8 (0.37) 3.8 (3.5 - 4.0)
Abs (at 420 nm; m^{-1})	0.4* -	1.4* -	0.9 (0.7) 0.9 (0.4 – 1.4)	2.6 (0.3) 2.6 (2.4 – 2.8)	- -	7.5* -	1.7 (0.2) 1.7 (1.5 – 1.8)	1.9 (0.4) 1.9 (1.6 – 2.1)	0.4* -	- -
Fe (µg L^{-1})	< 1.0* -	< 1.0* -	< 1.0** -	< 1.0** -	- -	< 1.0* -	< 1.0** -	< 1.0** -	< 1.0* -	< 1.0** -
Al (µg L^{-1})	< 1.0* -	< 1.0* -	< 1.0** -	< 1.0** -	- -	< 1.0* -	< 1.0** -	< 1.0** -	< 1.0* -	< 1.0** -
Mn (µg L^{-1})	< 1.0* -	< 1.0* -	< 1.0** -	< 1.0** -	- -	3.5* -	< 1.0** -	< 1.0** -	< 1.0* -	< 1.0** -
TP (µg L^{-1})	1.5* -	28* -	13 (0.33) 13 (13 - 14)	26 (13) 26 (17 - 35)	- -	25* -	12 (7.4) 12 (6.5 - 17)	12 (1.9) 12 (11 - 14)	18* -	16 (1.5) 16 (15 - 17)
TN (µg L^{-1})	545* -	942* -	695 (196) 695 (556 - 834)	512 (188) 512 (379 - 645)	- -	1320* -	947 (74.0) 947 (894 - 999)	213 (122) 213 (127 - 299)	< 15* -	< 15* -
NO_3^- (µg L^{-1})	339* -	115* -	196 (114) 196 (115 - 277)	163 (90) 163 (99 - 226)	- -	45* -	96 (24) 96 (79 - 113)	376 (68) 376 (328 - 424)	7* -	7* -
SO_4^{2-} (mg L^{-1})	4.3* -	15* -	4.4 (0.17) 4.4 (4.3 - 4.5)	120 (35) 120 (95 - 145)	- -	40* -	9.4 (0.29) 9.4 (9.2 - 9.6)	84 (20) 84 (67 - 98)	32* -	9.2 (0.42) 9.2 (8.9 - 9.5)
H_2S (mg L^{-1})	<0.10* -	<0.10* -	<0.10* -	<0.10* -	- -	<0.10* -	<0.10* -	<0.10* -	<0.10* -	<0.10* -
Si (mg L^{-1})	0.45* -	0.26* -	0.23 (0.13) 0.23 (0.13 - 0.32)	0.38 (0.09) 0.38 (0.31 - 0.44)	- -	0.25* -	0.67 (0.06) 0.67 (0.63 - 0.72)	0.36 (0.04) 0.36 (0.33 - 0.39)	0.14* -	0.22 (0.09) 0.22 (0.15 -0.28)

* Only one sample was collected.

** All values below detection limit.

*** One or several values below detection limit. Hence, means and standard deviations were not calculated.

S3. Summary of the physicochemical variables measured in the halocline of the blue holes. Top row in each cell show means with standard deviations within parenthesis, and the row below medians and ranges (min – max).

Variable	Cousteau's	East Twin	Hubcap	Ken's	Little Frenchman	Rainbow	Stalactite
DO (mg L^{-1})	0.44 (0.86) 0.06 (0.04 - 3.0)	0.09 (0.05) 0.07 (0.05 - 0.18)	0.09 (0.07) 0.06 (0.04 - 0.22)	2.8 (2.9) 3.0 (0.02 - 7.4)	2.2 (2.2) 2.0 (0.08 - 4.5)	0.05 (0.01) 0.05 (0.04 - 0.06)	0.19 (0.28) 0.06 (0.03 - 0.61)
Salinity (ppt)	13 (8.1) 10 (1.8 - 27)	12 (9.8) 10. (1.9 - 29)	9.7 (5.1) 9.9 (3.8 - 16)	18 (7.9) 19 (2.9 - 28)	3.9 (0.71) 3.9 (2.7 - 4.8)	18 (4.0) 16 (14 - 23)	21 (13) 22 (5.8 - 34)
Turbidity (FTU)	0.40 (0.20) 0.40 (0.02 - 0.81)	1.1 (1.2) 0.55 (0.14 - 3.0)	1.5 (1.3) 0.83 (0.33 - 3.1)	17 (41) 2.2 (0.49 - 126)	2.9 (1.3) 2.9 (0.83 - 5.0)	10.1 (18.0) 1.4 (0.63 - 37)	3.0 (2.8) 2.3 (0.41 - 7.0)
Temperature (°C)	24.9 (0.3) 25.0 24.2 - 25.1)	24.5 (0.1) 24.5 (24.4 - 24.6)	24.6 (0.7) 24.7 (23.8 - 25.4)	29.0 (1.4) 29.5 (25.8 - 30.1)	24.0 (0.3) 24.1 (23.4 - 24.4)	25.1 (0.4) 25.1 (24.6 - 25.6)	25.3 (0.4) 25.2 (25.0 - 25.9)
pH	7.7 (0.11) 7.6 (7.6 - 7.8)	7.9 (0.19) 7.9 (7.7 - 8.1)	7.6 (0.09) 7.6 (7.5 - 7.7)	- -	7.5 (0.14) 7.4 (7.4 - 7.7)	7.5 (0.23) 7.5 (7.4 - 7.7)	7.7 (0.13) 7.7 (7.6 - 7.8)
Chl a (µg L^{-1})	0.96 (0.45) 0.7 (0.68 - 1.48)	1.3 (1.1) 0.72 (0.56 - 2.55)	1.5 (1.1) 1.5 (0.8 - 2.3)	- -	25 (12) 25 (13 - 37)	23 (31) 23 (0.63 - 45)	5.8 (7.4) 5.8 (0.58 - 11)
Phycocyanin (µg L^{-1})	5.6 (3.4) 6.8(1.7 - 8.3)	2.3 (1.6) 1.9 (0.9 - 4.0)	3.3 (1.7) 3.3 (2.2 - 4.5)	- -	23 (3.0) 22 (21 - 26)	10 (9.9) 10 (3.1 - 17)	9.2 (4.4) 9.2 (6.1 - 12)
TOC (mg L^{-1})	2.0 (0.37) 2.0 (1.5 - 2.3)	4.1 (3.0) 2.5 (2.4 - 7.5)	2.2 (0.15) 2.2 (2.1 - 2.3)	- -	19 (1.5) 19 (18 - 21)	1.9 (0.06) 1.9 (1.8 - 1.9)	1.6 (0.70) 1.6 (1.1 - 2.1)
Abs (at 420 nm; m^{-1})	1.1 (0.9) 1.0 (0.3 – 2.1)	0.5* -	1.0 (0.3) 1.0 (0.8 – 1.2)	- -	6.0 (0.5) 5.9 (5.6 – 6.5)	1.4 (0.1) 1.4 (1.3 – 1.4)	0.7 (0.2) 0.7 (0.5 – 0.8)
Fe (µg L^{-1})	< 1.0** -	*** < 1.0 (< 1.0 - 45)	< 1.0** -	- -	*** 4.4 (< 1.0 - 21)	< 1.0** -	*** 60 (<1.0 - 120)
Al (µg L^{-1})	< 1.0** -	< 1.0** -	< 1.0** -	- -	*** < 1.0*	< 1.0** -	< 1.0** -
Mn (µg L^{-1})	21 (33) 5.1 (2.8 - 71)	22 (6.5) 20.3 (17.2 - 29.7)	5.9 (1.9) 5.9 (4.5 - 7.2)	- -	28 (6.4) 31 (21 - 32)	4.2 (1.4) 4.2 (3.3 - 5.2)	48 (33) 48 (25 - 72)
TP (µg L^{-1})	*** 13 (< 1.0 - 25)	19 (15) 16 (6.1 - 35)	49 (32) 49 (26 - 71)	- -	30 (2.4) 31 (27 - 31)	25 (5.4) 25 (21 - 29)	9.6 (11) 9.6 (1.6 - 18)
TN (µg L^{-1})	238 (213) 208 (26 - 511)	962 (514) 942 (458 - 1485)	1848 (715) 1848 (1342 - 2353)	- -	1220 (132) 1220 (1126 - 1313)	3518 (2818) 3518 (1525 - 5510)	342 (482) 342 (< 15 - 683)
NO_3^- (µg L^{-1})	132 (73) 115 (63 - 234)	178 (97) 158 (92 - 283)	84 (5) 84 (81 - 88)	- -	61 (18) 61 (48 - 74)	107 (4) 107 (104 - 110)	42 (51) 42 (7 - 78)
SO_4^{2-} (mg L^{-1})	501 (763) 158 (44 - 1643)	122 (101) 101 (33 - 232)	502 (146) 502 (399 - 605)	- -	133 (80) 166 (42 - 191)	1402 (246) 1402 (1228 - 1576)	899 (770) 899 (354 - 1443)
H_2S (mg L^{-1})	<0.10* -	0.06 (0.10) 0 (0 - 0.17)	1.3 (0.58) 1.3 (0.91 - 1.7)	- -	1.2 (1.5) 0.64 (0.13 - 3.0)	24 (20) 24 (10 - 38)	<0.10* -
Si (mg L^{-1})	0.52 (0.03) 0.51 (0.49 - 0.56)	0.56 (0.14) 0.62 (0.40 - 0.67)	0.33 (0.03) 0.33 (0.31 - 0.35)	- -	0.52 (0.08) 0.55 (0.43 - 0.59)	1.8 (1.2) 1.8 (1.2 - 2.6)	0.54 (0.24) 0.54 (0.37 - 0.71)

* Only one sample was collected.

** All values below detection limit.

*** One or several values below detection limit. Hence, means and standard deviations were not calculated.

S4. Summary of the physicochemical variables measured in the saline layer of the blue holes. Top row in each cell show means with standard deviations within parenthesis, and the row below medians and ranges (min – max).

Variable	Cousteau's	East Twin	Hubcap	Ken's	Little Frenchman	Rainbow	Stalactite
DO (mg L^{-1})	0.04 (0.01) 0.04(0.04 - 0.05)	0.04 (0) 0.04 (0.04 - 0.04)	0.05 (0.01) 0.05 (0.04 - 0.05)	0.02 (0.02) 0.01 (0 - 0.04)	0.06 (0.02) 0.07 (0.04 - 0.07)	0.02 (0.03) 0.02 (0 - 0.04)	0.02 (0.01) 0.03 (0.01 - 0.03)
Salinity (ppt)	36 (1.0) 37 (35 - 37)	36 (1.2) 37 (34 - 38)	22 (0.56) 22 (22 - 23)	37 (1.8) 37 (33 - 38)	15 (5.9) 15 (8.7 - 21)	27 (2.3) 27 (25 - 28)	34 (4.0) 36 (26 - 37)
Turbidity (FTU)	0.12 (0.02) 0.12 (0.10 - 0.14)	0.08 (0.04) 0.09 (0.04 - 0.12)	0.08 (0.03) 0.08 (0.06 - 0.10)	0.30 (0.18) 0.31 (0.08 - 0.52)	0.17 (0.13) 0.16 (0.04 - 0.30)	0.24 (0.05) 0.24 (0.20 - 0.27)	0.73 (0.37) 0.59 (0.37 - 1.35)
Temperature (°C)	24.5 (0.2) 24.5 (24.3 - 24.7)	24.5 (0) 24.5 (24.5 - 24.5)	25.3 (0) 25.3 (25.3 - 25.3)	26.1 (1.1) 25.7 (25.1 - 28.1)	25.6 (0.9) 25.6 (25.5 - 25.7)	25.7 (0.1) 25.7 (25.6 - 25.8)	25.0 (0.1) 25.0 (24.9 - 25.1)
pH	7.4 (0.01) 7.4 (7.4 - 7.4)	7.3* -	7.3* -	- -	7.3* -	7.4* -	7.3 (0.02) 7.3 (7.3 - 7.3)
Chl a (µg L^{-1})	0.55 (0.30) 0.55 (0.34 - 0.76)	0.18* -	0.50* -	- -	5.8* -	0.77* -	4.2 (5.3) 4.2 (0.48 - 7.9)
Phycocyanin (µg L^{-1})	5.8 (4.6) 5.8 (2.6 - 8.9)	- -	2.8* -	- -	8.7* -	3.2* -	3.3 (1.6) 3.3 (2.2 - 4.4)
TOC (mg L^{-1})	2.0 (0.13) 2.0 (1.9 - 2.1)	1.8* -	1.9* -	- -	9.3* -	1.8* -	1.9 (0.10) 1.9 (1.8 - 2.0)
Abs (at 420 nm; m^{-1})	0.6 (0.1) 0.6 (0.5 – 0.7)	0.6* -	1.6* -	- -	3.0* -	0.7* -	2.2 (0.9) 2.2 (1.5 – 2.8)
Fe (µg L^{-1})	< 1.0** -	< 1.0* -	< 1.0* -	- -	< 1.0* -	< 1.0* -	4.7 (6.5) 4.7 (0.10 - 9.3)
Al (µg L^{-1})	< 1.0** -	< 1.0* -	< 1.0* -	- -	< 1.0* -	< 1.0* -	< 1.0** -
Mn (µg L^{-1})	*** 1.3 (< 1.0 - 2.5)	3.3* -	8.2* -	- -	15* -	2.5 * -	5.1 (4.6) 5.1 (1.9 - 8.3)
TP (µg L^{-1})	4.7 (0.39) 4.7 (4.4 - 4.9)	3.2* -	8.9* -	- -	46* -	5.3* -	10 (13) 10 (< 1.0 - 20)
TN (µg L^{-1})	697 (25) 697 (680 - 716)	912* -	1606* -	- -	1245* -	5269* -	2614 (868) 2614 (2000 - 3228)
NO_3^- (µg L^{-1})	124 (33) 124 (101 - 148)	81* -	116* -	- -	73* -	90* -	79 (7) 79 (74 - 84)
SO_4^{2-} (mg L^{-1})	2367 (111) 2367 (2288 - 2445)	1460* -	1193* -	- -	245*	1877* -	1735 (119) 1735 (1651 - 1820)
H_2S (mg L^{-1})	4.9 (6.8) 4.9 (0.11 - 9.7)	4.5* -	10* -	- -	7.0*	38* -	16 (8.8) 16 (9.9 - 22)
Si (mg L^{-1})	0.47 (0.02) 0.47 (0.46 - 0.48)	0.49* -	1.0* -	- -	0.67*	2.5* -	1.2 (0.28) 1.2 (1.0 - 1.4)

* Only one sample was collected.

** All values below detection limit.

*** One or several values below detection limit. Hence, means and standard deviations were not calculated.